

# One-dimensional metastructures composed of cables with scatter masses: waves, vibrations and band gaps

Marco Moscatelli<sup>1,2,a\*</sup>, Claudia Comi<sup>1,b</sup> and Jean-Jacques Marigo<sup>2,c</sup>

<sup>1</sup>Department of Civil and Environmental Engineering, Politecnico di Milano, Milano, Italy

<sup>2</sup>Laboratoire de Mécanique des Solides, École Polytechnique, Palaiseau, France

<sup>a</sup>marco.moscatelli@polimi.it, <sup>b</sup>claudia.comi@polimi.it, <sup>c</sup>jean-jacques.marigo@polytechnique.edu

**Keywords:** Metamaterials, Cable Dynamics, Wave Attenuation

**Abstract.** This work analyzes the dynamic behavior of structural elements that can be modelled as taut cables with a discrete array of punctual attached and hanging masses. The propagation of mechanical waves is strongly influenced by the presence of such scatter elements. We found that the problem is governed by a discrete equation, whose solutions depend on the behavior of an equivalent mass density, that varies with frequency. The spectrum of the problem is characterized by the presence of band gaps. This behavior is generally exploited for the design of metastructures. A parametric study of the equivalent mass is finally given.

## Introduction

Long and flexible slender elements are typically modelled as cables, i.e. as structures with no flexural rigidity. The dynamics of such systems has been widely studied due to the possible activation of several peculiar mechanisms mainly connected to the intrinsic non-linearities of the problem [1–3].

In most applications, cabling systems present hanging elements that are often periodically repeated. This is the case for instance for the main cables in suspension bridges [4], for cableways [5] and for overhead lines with ball markers or vibrational dissipators [6]. These elements largely influence and modify the dynamic response of the system, acting as scatterers for propagating waves. To show this, we here analyze a simplified problem by studying the propagation of mechanical waves in taut cables with a periodic array of masses, directly attached to the cable or/and hanging to it by means of elastic springs. We focus on the linear dynamics of the system. Specifically, we verified that there exist some intervals of frequencies at which waves cannot propagate through the cable, i.e. band gaps in the spectrum. We thus found that the system can behave as a metastructure.

In this work, we initially derive an equivalent equation governing the linear dynamics of our system and we show that band gaps can indeed appear. We then analyze how these band gaps are modified by a variation of the parameters involved in the problem: this analysis gives useful information for the design phase.

## Problem formulation

Let us analyze the propagation of transverse mechanical waves in taut cables. This model can be used to study the behavior of long and slender structural elements, characterized by a low flexural rigidity, that are stretched between two supports positioned at the same height. The cable is here characterized by the presence of a periodic arrangement of pointwise hanging elements, composed of masses  $m_1$  directly attached to the cable and connected to hanging masses  $m_2$  by means of elastic springs  $k$  (cf. Fig. 1).



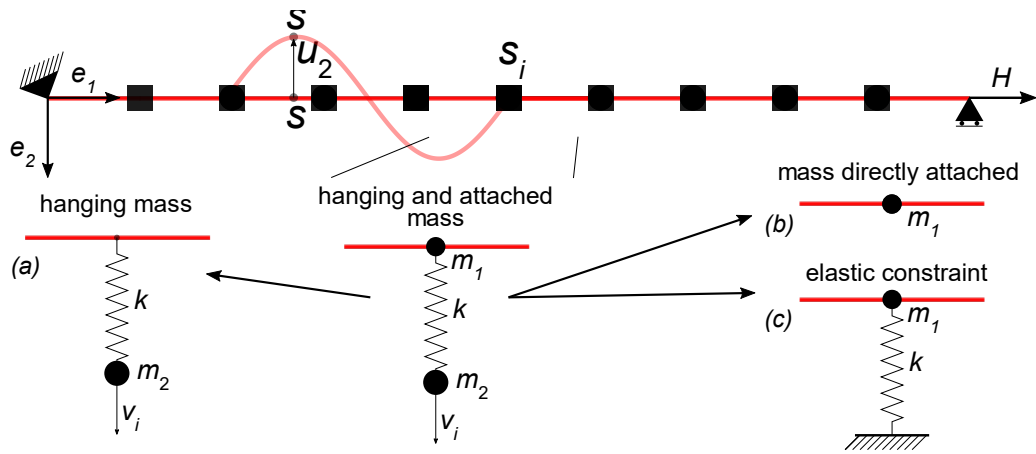


Figure 1: Cable in tension under a force  $H$ , with a periodic distribution of scatter elements composed of masses  $m_1$  directly attached to the cable and/or masses  $m_2$  hanging through springs  $k$ . The following limiting cases are shown: in scheme (a) masses are hanging to the cable by means of elastic springs, in scheme (b) masses are directly attached to the cable, and in scheme (c), masses are constrained to the ground by means of elastic springs. Direction  $e_3$  is out-of-plane.

By calling  $H$  the pretension applied to the cable, the equilibrium configuration can be approximated to be horizontal when  $H$  is much larger than the total weight of cable and attached elements. Specifically, a material point  $s_0$  will be moved to a different position  $s$ , during this pretensioning phase, along direction  $e_1$  (see Fig. 1). By calling  $N_{eq}(s_0)$  the axial force and  $\epsilon_{eq}(s_0)$  the static axial strain of the point originally at position  $s_0$ , from equilibrium and linear elasticity one has

$$N_{eq}(s_0) = H \quad \text{and} \quad \epsilon_{eq}(s_0) = H/EA, \tag{1}$$

where  $EA$  is the axial stiffness of the cable.

Note that, with the current assumptions, the presence of the punctual elements does not influence the static equilibrium of the system. This is not the case when the cable is moving. To show this, let us now take the static equilibrium configuration to be the new reference configuration for the dynamic problem. We call  $L$  the distance between the two supports and  $n$  the total number of hanging elements. Accordingly,  $d = L/(n + 1)$  is the distance between two subsequent elements. As we are dealing with a wave propagation problem, we do not consider the boundary conditions.

By studying small oscillations around the equilibrium configuration, the motion problem is governed by three uncoupled equations along the in-plane horizontal and transverse directions and the out-of-plane direction (respectively, directions  $e_1$ ,  $e_2$  and  $e_3$  in Fig. 1). Specifically, along the transverse direction  $e_2$ , one has:

$$\ddot{u}(s, t) - c_t^2 u''(s, t) = 0 \quad \forall s \notin P \tag{2}$$

where we use  $(\ddot{\blacksquare})$  and  $(\blacksquare)''$  to denote respectively the time and spatial derivatives. In Eq. 2,  $c_t^2 = EA(1 + \epsilon_{eq})^2 / \rho$  is the speed of transverse waves, and we have used  $P$  to define the collection of positions  $s = s_i$  of the  $i$ -th hanging elements. The motion problem is then completed by a set of jump conditions, such that:

$$\llbracket EA\epsilon_{eq}u' \rrbracket (s_i, t) = m_1 \ddot{u}(s_i, t) - k(v_i(t) - u(s_i, t)) \quad \text{with } 1 < i < n, \tag{3}$$

where  $\llbracket \blacksquare \rrbracket = (\blacksquare)^+ - (\blacksquare)^-$ , with  $(\blacksquare)^+$  (resp.  $(\blacksquare)^-$ ) denoting the right (resp. left) limit of  $(\blacksquare)$  at  $s$ . In the above Eq. 3, we used  $v_i$  to denote the vertical displacement of the end point of the spring

where the mass  $m_2$  of the  $i$ -th element is attached, by making the assumption that these masses can only move in the vertical direction  $\mathbf{e}_2$ . Accordingly, the equation of the vertical motion of the  $i$ -th mass  $m_2$  reads as:

$$m_2 \ddot{v}_i + k(v_i(t) - u(s_i, t)) = 0. \quad (4)$$

Note that Eq. 3 can be also used to model the case when masses  $m_1 + m_2$  are directly attached to the cable and the case when the elastic springs are constrained to the ground. For this, one has to consider, respectively, an infinite stiffness  $k$  and an infinite mass  $m_2$ . Specifically, from Eq. 4, one has for the former case  $v_i(t) = u(s_i, t)$ , meaning that the system behaves as if masses  $m_2$  were directly attached to the cable and summed to masses  $m_1$ . For the latter case, instead, one has  $\ddot{v}_i = 0$ , meaning that masses  $m_2$  cannot move. These cases are shown in Fig. 1 (schemes (b) and (c)), together with the case corresponding to  $m_1 = 0$  (scheme (a)).

By considering that both fields  $u$  and  $v_i$  are small and harmonically varying in time, such that

$$u(s, t) = \hat{u} L \exp i\omega t \quad \text{and} \quad v_i(s, t) = \hat{v}_i L \exp i\omega t, \quad (5)$$

Eq. 2 can be solved within each interval  $i$ -th. The term  $i$  is used in relations 5 and in the followings to denote the imaginary unit. By calling  $\hat{u}_i$  the transverse displacement of the  $i$ -th mass  $m_1$ , one obtains

$$\hat{u}(\hat{s}) = \hat{u}_{i-1} \cos(\Omega(n+1)\hat{s} - i + 1) + \frac{\hat{u}_i - \hat{u}_{i-1} \cos \Omega}{\sin \Omega} \sin(\Omega(n+1)\hat{s} - i + 1) \quad (6)$$

where  $\Omega = \omega d/c_t$  and  $\hat{s} = s/L$  are respectively dimensionless frequency and coordinate. Using Eq. 6, together with Eq. 3 and 4, one finally finds the following equivalent equation of motion for the points  $s_i \in P$ :

$$\Delta_i \hat{u} + \mu(\Omega) \hat{u}_i = 0, \quad \text{with} \quad \Delta_i \hat{u} = \hat{u}_{i+1} + \hat{u}_{i-1} - 2 \hat{u}_i. \quad (7)$$

In the above equation,  $\mu(\Omega)$  can be interpreted as a frequency dependent equivalent mass density and it reads

$$\mu(\Omega) = 2(1 - \cos \Omega) + \left( \Theta_1 + \frac{\hat{k} \Theta_2}{\hat{k} - \Theta_2 \Omega^2} \right) \Omega \sin \Omega \quad (8)$$

where  $\Theta_1$  and  $\Theta_2$  are two mass ratios and  $\hat{k}$  is a normalized stiffness of the springs:

$$\Theta_1 = \frac{m_1}{\rho d}, \quad \Theta_2 = \frac{m_2}{\rho d}, \quad \text{and} \quad \hat{k} = \frac{k d}{N_{eq}}. \quad (9)$$

### Spectral band gaps

From the derivation in [7], one has the following solutions of Eq. 7:

$$\begin{aligned} \hat{u}_i &= A \exp(-i K^* i) + B \exp(i K^* i) && \text{for } 0 \leq \mu(\Omega) \leq 4, \\ \hat{u}_i &= A \exp(-K^* i) + B \exp(K^* i) && \text{for } \mu(\Omega) < 0, \\ \hat{u}_i &= A (-1)^i \exp(-K^* i) + B (-1)^i \exp(K^* i) && \text{for } \mu(\Omega) > 4, \end{aligned} \quad (10)$$

where  $K^* \in [0, \pi]$  is a dimensionless wavenumber obtained as:

$$1 - \frac{\mu(\Omega)}{2} = \begin{cases} \cos K^* & \text{for } 0 \leq \mu(\Omega) \leq 4, \\ \cosh K^* & \text{for } \mu(\Omega) < 0, \\ -\cosh K^* & \text{for } \mu(\Omega) > 4. \end{cases} \quad (11)$$

Accordingly, waves propagate freely along the cable when  $0 \leq \mu(\Omega) \leq 4$ . For either  $\mu(\Omega) < 0$  or  $\mu(\Omega) > 4$ , waves are instead attenuated, as the displacement field is given by a superimposition of exponentials.

The spectrum of the problem governed by Eq. 7 is thus characterized by *band gaps*, i.e. by intervals of frequencies at which wave solutions does not exist.

### Parametric study of band gaps

As discussed in the previous section, band gaps are given by those frequencies at which either  $\mu(\Omega) < 0$  or  $\mu(\Omega) > 4$ . Considering for example the case with  $\Theta_1 = 0$ ,  $\Theta_2 = 1.18$  and  $\hat{k} = 4$  (hanging masses), we report in Fig. 2 the behavior of  $\mu$  in function of the frequency  $\Omega$ . Band gaps are denoted by the green ( $\mu(\Omega) < 0$ ) and red ( $\mu(\Omega) > 4$ ) intervals. Blue intervals correspond to pass bands.

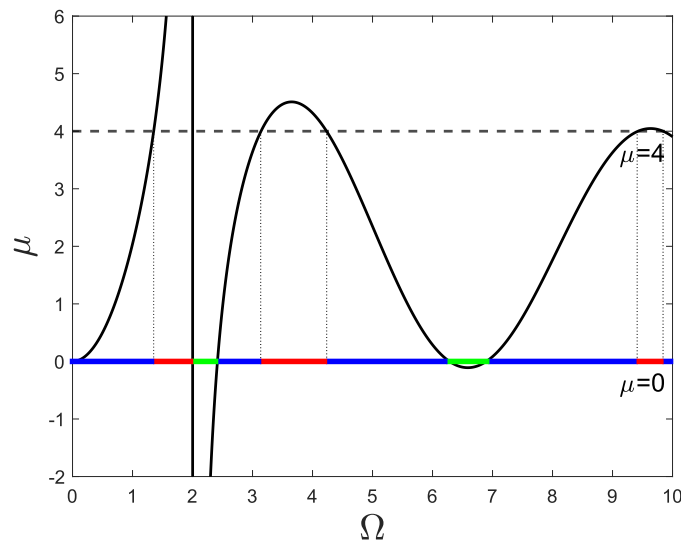


Figure 2: Equivalent mass vs frequency for the system studied in Fig. 5, with  $\hat{k} = 4$ . Colors must be interpreted as in Figures 3 to 6: blue is used for pass bands, red and green for band gaps.

Let us now study how the equivalent mass density  $\mu(\Omega)$  is influenced by the parameters given by relations 9. Specifically, we here analyze how band gaps vary in function of them. For this, we show some contour plots (Figures 3 to 6) of the equivalent mass  $\mu(\Omega)$  for the following cases:

Fig. 3. Cable with masses  $m_1$  and no hanging mass ( $m_2 = 0$ ).

Fig. 4. Cable with  $m_1 = 0$  and  $m_2 \rightarrow \infty$  (cable lying on a discrete array of elastic constraints).

Fig. 5. Cable with  $m_1 = m_2 = m$  ( $\Theta_1 = \Theta_2 = \Theta$ ) and fixed dimensionless spring stiffness  $\hat{k}$ .

Fig. 6. Cable with hanging masses  $m_2$  ( $m_1 = 0$ ) and varying dimensionless spring stiffness  $\hat{k}$ .

As before, in the contour plots the conditions  $\mu(\Omega) < 0$  and  $\mu(\Omega) > 4$  are verified respectively in the green and red regions. The blue areas, instead, correspond to pass bands.

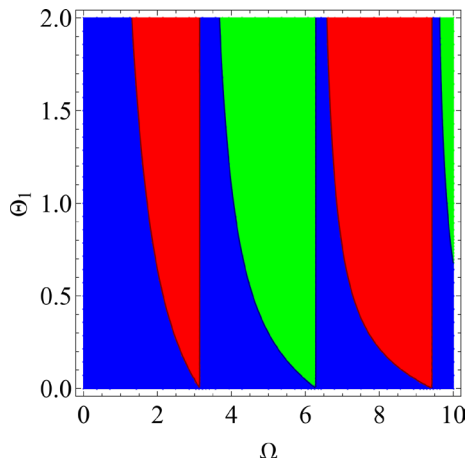


Figure 3: Masses directly attached to the cable for varying mass  $m_1$  ( $m_2=0$ ).

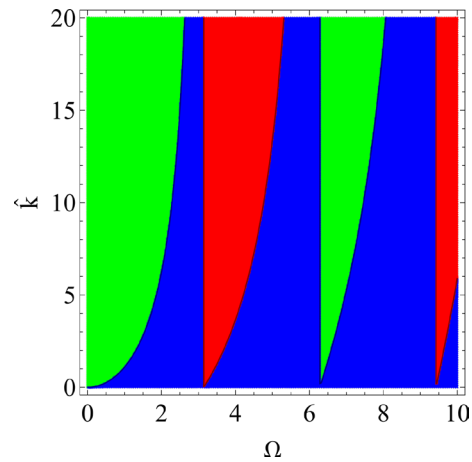


Figure 4: Cable lying on a discrete set of elastic springs for varying stiffness ( $m_1=0$ ).

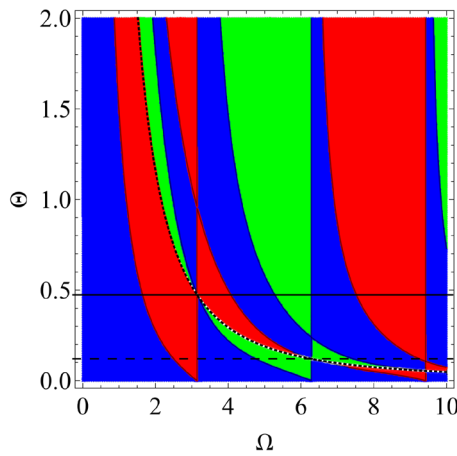


Figure 5: Cable with equal attached and hanging masses for varying mass  $m_1=m_2=m$ . For this plot we used  $\hat{k} = 4.73$ .

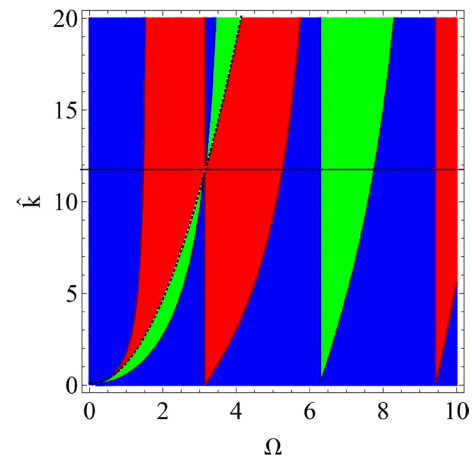


Figure 6: Cable with hanging masses for varying stiffness  $k$  ( $m_1=0$ ). For this plot we used  $\theta_2 = 1.18$ .

Note that the system studied in Fig. 2 corresponds to that used in Fig. 6, by fixing  $\hat{k} = 4$ . Colors have the same meaning in both Figures.

From Fig. 3, the width of band gaps increases with the mass. For the system analyzed in Fig. 4, their width increases with the stiffness. Most importantly, this latter case is characterized by a cut-off frequency with a band gap opening at zero frequency. Note that the closing frequencies in Fig. 3 and the opening frequencies in Fig. 4 are independent respectively from a variation of attached mass and stiffness. This can be explained by studying the behavior of the equivalent mass  $\mu$ . For this, let us first rewrite here relation 8 for these two cases

$$\mu(\Omega) = \begin{cases} 2(1 - \cos \Omega) + \theta_1 \Omega \sin \Omega \\ 2(1 - \cos \Omega) + \hat{k} \frac{\sin \Omega}{\Omega} \end{cases} \quad (12)$$

From relations 12 one can recognize that at points  $j\pi$ , with  $j \in \mathbb{N}_*$ , the first and second terms in the definition of the equivalent mass are both zero independently of  $\theta_1$  and  $\hat{k}$ .

Let us now comment on Figures 5 and 6. In both cases, the systems used are characterized by the presence of resonant elements (springs and masses  $m_2$ ) that can locally resonate causing the opening of band gaps. The dotted black curves in these contour plots show how the resonance

frequency varies with respect to the varying parameters. Specifically, the equivalent mass is indefinite at resonance and tends to  $+\infty$  or  $-\infty$  from below or from above (cf. Fig. 2), depending on the case under consideration. Accordingly, band gaps will always appear around the frequency of resonance, as one can check from the contour plots. From Fig. 6, band gaps width clearly increases with the stiffness. The presence of opening and closing frequencies that result to be independent from a variation of mass (Fig. 5) and stiffness (Fig. 6) can be explained by looking at the equivalent mass  $\mu$  with a reasoning similar to that followed for Figures 3 and 4.

Note that, for the parameters fixed by the black continuous horizontal lines in Figures 5 and 6, the two systems are characterized by a spectrum where the closing frequency of the first band gap is superimposed with the opening frequency of the second band gap: the final band gap becomes thus very wide, resulting in an optimal attenuating behavior. This feature is also valid for the second and third band gaps in the spectrum shown in Fig. 5, as indicated by the black dashed horizontal line.

## Conclusions

In this paper we have considered the linear dynamic behavior of a cable with hanging elements. We found that this system behaves as a metastructure, offering the peculiar property that waves cannot freely propagate for some intervals of frequencies, generally known as band gaps. For this, we have derived an equivalent mass density from which we were able to obtain information regarding the influence of the parameters involved in the problem. The result can be of interest as a starting point for more realistic models where the initial sag of the cable is taken into account. This would better idealize the structural applications listed in the introduction of the current work. Moreover, the attenuating capabilities of the system could be exploited for the localization and focusing of mechanical waves, as shown in [8,9].

## References

- [1] M. Irvine, Cable structures, The Massachusetts Institute of Technology, Cambridge, 1981.
- [2] S.A. Nayfeh, A.H. Nayfeh, D.T. Mook, Nonlinear Response of a Taut String to Longitudinal and Transverse End Excitation, *Journal of Vibration and Control*. 1 (1995) 307–334. <https://doi.org/10.1177/107754639500100304>
- [3] A.H. Nayfeh, H.N. Arafat, C.-M. Chin, W. Lacarbonara, Multimode Interactions in Suspended Cables, *Journal of Vibration and Control*. 8 (2002) 337–387. <https://doi.org/10.1177/107754602023687>
- [4] F. Gazzola, *Mathematical Models for Suspension Bridges*, Springer International Publishing, Milan, 2015. <https://doi.org/10.1007/978-3-319-15434-3>
- [5] J.M.W. Brownjohn, Dynamics of an aerial cableway system, *Engineering Structures*. 20 (1998) 826–836. [https://doi.org/10.1016/S0141-0296\(97\)00113-2](https://doi.org/10.1016/S0141-0296(97)00113-2)
- [6] F. Foti, V. Denoël, L. Martinelli, F. Perotti, A stochastic and continuous model of aeolian vibrations of conductors equipped with stockbridge dampers, in: *Proceedings of the International Conference on Structural Dynamic , EURODYN, European Association for Structural Dynamics, 2020*: pp. 2088–2102. <https://doi.org/10.47964/1120.9169.20304>
- [7] M. Moscatelli, C. Comi, J.J. Marigo, On the dynamic behaviour of discrete metamaterials: From attenuation to energy localization, *Wave Motion*. 104 (2021) 102733. <https://doi.org/10.1016/j.wavemoti.2021.102733>
- [8] M. Moscatelli, *Metamaterials for energy harvesting at small scale*, École polytechnique, 2022.
- [9] M. Moscatelli, C. Comi, J. Marigo, Attenuation and localization of waves in taut cables with a discrete array of scatter elements, in: *Proceedings ECCOMAS, 2022*. <https://doi.org/10.23967/eccomas.2022.057>